



# Optimum Sublevel Height and Drift Spacing in Sublevel Cave Mining Based on Random Medium Theory

Kunpeng Yu<sup>1,2</sup> · Fengyu Ren<sup>1</sup> · Gideon Chitombo<sup>2,3</sup> · Ruslan Puscasu<sup>2,3,4</sup> · Liangliang Kang<sup>5</sup>

Received: 3 October 2019 / Accepted: 7 January 2020 / Published online: 14 January 2020  
© Society for Mining, Metallurgy & Exploration Inc. 2020

## Abstract

Weak rock mass and poor flow of material can cause excessive ore loss and dilution in sublevel caving. This paper proposes a method to establish design parameters for an inclined deposit within a weak rock mass and evaluates its effectiveness through a case study. In order to solve the problem of low production capacity and poor safety conditions of sublevel caving mining at the Yingfangzi silver mine in China and to ensure a smooth production from the refractory ore body, it is necessary to select appropriate stope structure parameters. Based on random medium theory of gravity flow and the improved equation of ore discharge in random medium, an end wall drawing experiment is carried out to determine the optimum design and flow parameters. It was observed from the experiment that, due to the influence of the randomness of particle movement, there is a mismatch in the flow parameter measurement. The flow characteristics and distribution of the marker particles are different from that of the tested particles resulting in large drawbody shape distortion. The study finds that the flow parameters obtained by the new method are more practical and account for drawpoint width and recommends that the new method for determining the sublevel stope height is used when the drawbody is a non-standard ellipsoid. The outcomes have shown a significant reduction in the dilution and improvement in the recovery rates, and the safety and efficiency of mining have been greatly improved.

**Keywords** Random medium theory · Sublevel caving · Sublevel height · Drift spacing · Stope structure parameters

## 1 Introduction

With the diminishing mining resources and increasingly complex geological settings, the productivity decline of metal mines across the world is becoming a significant challenge [1, 2]. Achieving safe and efficient mining under extreme geotechnical conditions is a frequently encountered problem in mining design [3–5]. Contemporary sublevel caving, originally developed in the Swedish iron mines, is a widely used

mass mining method in metallic mines across the world [6–8]. This method has many advantages in terms of mechanization and safety. As production is carried out only in drifts that can be well supported, the safety of this method is relatively better than of other mining methods such as room-and-pillar and cut-and-fill [9]. For this reason, as well as because of its high mechanizability, sublevel caving is becoming the option of choice in China and other countries for mineral deposits amenable to caving [10, 11]. However, the relatively high development cost of sublevel caving and the dilution and its control, particularly in inclined orebodies under complex geological conditions, are significant factors that need to be considered in any sublevel cave design [12, 13]. The optimal design parameters are the most important performance criteria for the dilution loss, which can also directly influence the continuous operation performance of the total mining system [14]. Reliability analysis of sublevel design parameters can be performed to calculate its optimal design parameters [19, 21, 22] as well as three-dimensional numerical modeling to predict the dilution loss under certain design parameters [18, 20, 26]. The key design parameters considered in these models include sublevel height, drift spacing and ring burdens. In order to ensure the optimized design parameters, the sublevel

✉ Kunpeng Yu  
yukunpengyx@163.com

<sup>1</sup> School of Resources and Civil Engineering, Northeastern University, Shenyang 110819, China

<sup>2</sup> Sustainable Minerals Institute, The University of Queensland, St Lucia, QLD 4072, Australia

<sup>3</sup> Mining3, Pinjarra Hills, QLD 4069, Australia

<sup>4</sup> CSIRO Mineral Resources, Queensland Centre for Advanced Technologies, Pullenvale, QLD 4069, Australia

<sup>5</sup> Patent Examination Cooperation Hubei Center of the Patent Office, Wuhan 430070, China

height need to be determined first, followed by drift spacing and finally the ring burdens [15–17].

Sublevel cave mining production relies on gravity flow models that capture the geometry of the caved ore as well as the fundamental phenomena governing the flow of caved material. The physical and mechanical parameters of particles, such as size, distribution and uniformity, have certain influence on the draw. The movement of individual particle tends to be random and flow characteristics tend to be highly irregular. At the same time, pulsation and asymptotic failure exist in the process of ore drawdown, which present great difficulties in explicit mathematical modeling and calculations of flow related processes. Because of the relative randomness of the movement of rock particles, one can regard the caved volume as a medium material with probabilistic factors and can use probability theory to describe its movement. The domain can then be simplified as a random medium with continuous flow and examined within so called random medium theory of ore flow.

In this paper, firstly, a flow parameter analysis of the particles is carried out. The placement method of the marker particles is improved and a new method for measuring the flow parameters of the particles is suggested by using the ‘discharge equation’, which describes the relationship between the released quantity and the shape the drawbody. Drawbody is defined as a surface formed by the movement of particles that reach the drawpoint. The equations of movement velocity and trace line of the continuous particle medium are derived according to the central limit theorem. The method is applied to the production of Yingfangzi silver mine. The flow parameters measurement tests of Yingfangzi ores is carried out, and the results of the measurement method are analyzed. Consequently, through the above work, the engineering applicability of random medium gravity flow theory is tested, analyzed and improved.

Secondly, if the drift height is kept constant, increasing the section width of the drawing point is conducive to improving the flow performance of ores and subsequently ore recovery. Therefore, on the basis of above experiments, the effect of drawpoint size on the recovery is analyzed and the random medium theory of flow is further enhanced. Furthermore, a new method for determining structural parameters of sublevel caving stope is put forward.

### 1.1 The Yingfangzi Silver Mine Deposit

The Yingfangzi mine is located within Yingfangzi village of Fengning city, Hebei province, in north China,  $41^{\circ}36' N$  longitude and  $116^{\circ}31' E$  latitude, covering an area of approximately  $1.2 \text{ km}^2$ . The mine area’s elevation ranges from 1200 to 1500 m above sea level (asl). It has a continental monsoon climate, with warm temperatures and distinct seasons. The annual average precipitation is about 350 mm. The geological

exploration of the area was completed by the No. 514 Geological Party of Hebei province in 1993.

Yingfangzi silver mine is one of the first sublevel caving mines developed in China. The deposit has a weak and jointed rock mass and a gentle dip angle. In this work, the appearance law of underground stresses, the rule of rock mass caving and the medium flow pattern were applied, respectively, to work out the optimal height of sublevel and the drift spacing that correspond to Yingfangzi silver mine. The test design parameters were selected within the deposit 142<sup>#</sup>–47<sup>#</sup> prospecting line, vertical elevation between 1010 and 1130 m levels. The orebody is low to the northeast, high to the southwest (see Fig. 1). On average, its dip angle is  $50^{\circ}$  but gentler in the middle around  $35^{\circ}$ . Its average thickness is 18 m. The main roof of surrounding rocks of the ore body is breccia, mudstone and gneiss. The floor is composed of breccia and granite. The orebody mainly consists of galena, sphalerite and pyrite, in which all of these components contain silver. The main features of the ore-body are: simple design, large number of joints and cracks, soft broken rock with bad stability, basal quality indexes of rock mass from 162 to 310 (*BQ index*) and a great quantity of powder ore. The minerals have the tendency to form mudflow. Given its ore characteristics, the Yingfangzi deposit is suitable for analysis within the framework of random medium theory.

## 2 The Random Medium Theory of Gravity Flow

The theory of ore flow in random medium abstracts the particles into continuous flowing random medium and employs probability theory to study the movement of ore particles. Combining the method of random medium with the actual physical process of gravity flow, the theoretical equation of the system was established based upon the particles movement under the boundary conditions of the experiment. The two parameters ( $\alpha$  and  $\beta$ ) reflecting the flowing characteristics of the particle flow were introduced to make the shape of the

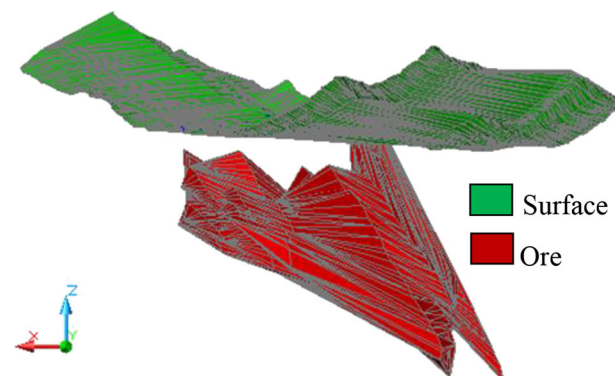


Fig. 1 Perspective view of the Yingfangzi silver mine deposit

flow better match the observations and optimize the structural parameters of the stope. The flow parameters  $\alpha$  and  $\beta$  in the random medium theory of gravity flow are the first design parameters to be determined in the field production application. These flow parameters are obtained by physical (laboratory) simulation and industrial (field) testing. Because the flow parameters obtained by industrial testing are similar to the results obtained by physical simulation of gravity flow in the laboratory, most mines (especially new ones) still conduct physical simulations.

The theoretical basis of the physical simulation of ore drawing is described by the relationship between the released quantity and the height of the drawbody, i.e.

$$Q = \frac{\beta}{\alpha + 1} \pi H^{\alpha+1} \tag{1}$$

where  $\alpha$  and  $\beta$  are the particle flow parameters during bottom ore drawing;  $Q$  is release quantity;  $H$  is the height of drawbody. Marker particles are arranged in layers at a certain height with a distance of 0 from the drawpoint center, and then the quantity  $Q$  of the marker particles when they reach the drawpoint is measured, and the parameters ( $\alpha$  and  $\beta$ ) are obtained by statistical regression.

The current measurement method of flow parameters in random medium theory has the following shortcomings: firstly, due to the uncertainty and randomness of the movement of particles [18], the marker particles arranged at a certain point may not be released even after ore drawing is completed, or the marker particles that should be released first may be released later, thus resulting in distortion of the obtained parameters. Secondly, the marker particles are generally synthetic particles, not from the sample particle set. The mechanical properties of marker particles are different from that of test particles in terms of humidity, density, cohesion, friction angle and other mechanical properties. Thirdly, the gradation of labeled particles and test particles is inconsistent.

The theory of random medium ore drawing regards loose ore rock as a kind of ‘random medium’, and the process of loose ore rock release as a random process. From a statistical point of view, it describes the internal movement law of the particle, that is, the particle moves from the position with a small probability to the position with a large probability. As shown in Fig. 2, when point source ore drawing, the descending probability of any point  $(r, Z)$  above the ore drawing point is  $p$ :

$$p(r, Z) = \frac{1}{\sqrt{\pi\beta Z^\alpha}} e^{-\frac{r^2}{\beta Z^\alpha}} \tag{2}$$

where  $\alpha$  and  $\beta$  are the flow parameters of the particles,  $Z$  is the height of the particle point. It is assumed that the discharge amount per unit time at the drawpoint is  $q$ , and, in the moving

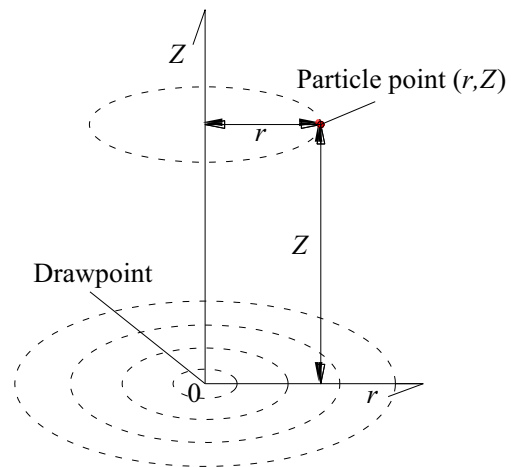


Fig. 2 Spatial coordinate system for particle drawdown

band, the moving velocity of particles at any position is proportional to the moving probability at this point. If movement of particles meets the condition of passive continuous flow field, then the moving velocity equation of particles can be written as

$$\begin{aligned} v_Z &= -\frac{q}{\pi\beta Z^\alpha} e^{-\frac{r^2}{\beta Z^\alpha}} \\ v_r &= -\frac{\alpha q r}{2\pi\beta Z^{\alpha+1}} e^{-\frac{r^2}{\beta Z^\alpha}} \end{aligned} \tag{3}$$

where  $v_Z$  and  $v_r$  are respectively the flow velocity of the particle in the vertical direction and the horizontal direction during bottom ore drawing;  $q$  is the loose volume released per unit time at the drawpoint and is a constant. After the velocity field is determined, the equations of particle moving path, releasing drawbody, moving funnel and releasing funnel can be obtained.

### 3 The Effect of Draw Point Size on Particle Movement

The simulated drawing experiment model is cuboid, the size of the drawing experimental model is  $25 \times 27 \times 40$  cm, and the particles are dolomite with a size of 2~6 mm. The particles are in the state of natural accumulation, and the loading density is  $1.6548 \text{ g/cm}^3$ . Two marker particles are placed every 5 cm on the central axis of the ore drawing orifice, and a total of 7 layers are arranged. The corresponding discharge amounts of different ore drawing orifice sizes are sampled five times as replicates. The particles released volume as a function of particle released height is shown in Fig. 3. The error bars represent standard deviations of replicates. It can be seen from Fig. 3 that the size of ore draw opening has an obvious influence on the released number of particles. With the increase of the release height, the release amount of the particles

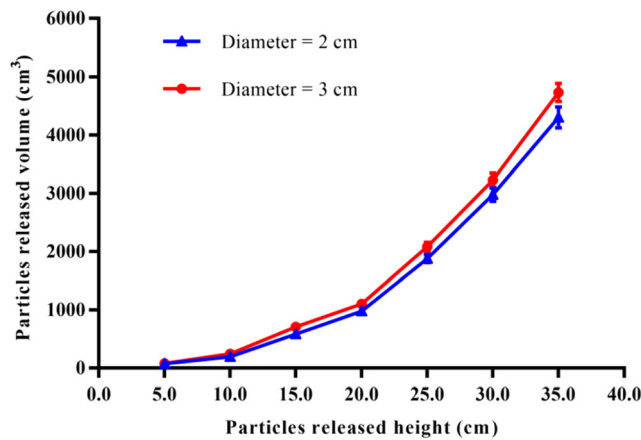


Fig. 3 Relationship between drawpoint diameter (*D*) and particles released volume in experiment

increases at different drawpoint diameters (2 and 3 cm). Under the condition of the same release height, the release amount of particles when the diameter of the drawpoint is 3 cm is greater than that when the diameter of the drawpoint is 2 cm. Hence at the same release height, the release amount increases as drawpoint size increases.

In order to study the relationship between the drawpoint size and the flow parameter value of particles, four experiments with different drawpoint sizes were carried out for the same type of particles. The experimental results are presented in Table 1. As can be seen from Table 1, with the increase of ore drawpoint size, the flow parameter  $\alpha$  decreases and the value  $\beta$  increases. In Table 1, the value of the regression coefficient decreases with the increase of ore draw point radius, which indicates that the flow parameters  $\alpha$  and  $\beta$  are not only affected by the size of ore drawpoint but also by the ore drawing boundary conditions and other factors.

By increasing the size of ore drawpoint, the flow state of the particles is more stable, the curve of the movement probability density of the particles becomes relatively flat, and the curvature radius of the curve near the flow axis increases. Therefore, a larger drawpoint is conducive to a stable decline of top rock and therefore to a more controlled dilution. When drawing ore, the whole section of the ore drawpoint must be kept uniform, which can make the ore and rock drawing layer more even, so as to reduce the contact area between the caved ore and the top overburden waste rock, which is beneficial in reducing ore dilution and loss.

Table 1 Experimental relationship between size of drawpoint (radius) and particle flow parameters

Drawpoint radius	Regression equation for <i>Q</i> and <i>H</i>	Related coefficient	$\alpha$	$\beta$
0.75	$Q = 0.349H^{2.562}$	0.9995	1.562	0.2846
1.00	$Q = 0.5287H^{2.469}$	0.9975	1.469	0.4155
1.25	$Q = 1.1474H^{2.27}$	0.9940	1.270	0.8291
1.50	$Q = 1.2207H^{2.26}$	0.9940	1.260	0.8781

### 4 Improved Equation of Ore Flow in Random Medium

The basic equation of the above random medium flow theory is obtained under the assumption that the width of the drawpoint is 0. In practice, the width of the drawpoint is not 0, as shown in Fig.4. Therefore, it is necessary to improve the basic equation of the random medium flow theory to account for drawpoint width. Let us assume that the width of the drawpoint is *D*,  $\theta$  is the angle of the straight-line trajectory of the particle (measured from the horizontal direction), the straight-line trajectory of the particle  $\theta = 90^\circ$  and  $\theta = \theta_G$  extend downward and intersect at a point (as depicted in Fig. 4). In this case, the vertical distance between the intersection point and the top of the drawpoint is *H*<sub>0</sub>, and its value can be defined as

$$H_0 = \frac{D}{2} \tan \theta_G \tag{4}$$

where the angle  $\theta_G$  is assumed to be dependent on the internal friction angle  $\varphi_0$ , and satisfies the following relation:

$$\theta_G = \frac{\pi}{4} + \frac{\varphi_0}{2} \tag{5}$$

The internal friction angle varies with particle size and roughness. The rougher the particle is, the higher its value is. The polar equation of the released particles is written as

$$r^2 = (\alpha + 1)\beta Z^\alpha \ln \frac{H + H_0}{Z} \tag{6}$$

According to the above formula, the volume of the released particles can be obtained by integrating the horizontal micro-disc depicted in Fig. 2. If the volume of the element disk is

$$dV = \pi r^2 dZ = \pi(\alpha + 1)\beta Z^\alpha \ln \frac{H + H_0}{Z} dZ \tag{7}$$

Then the volume of the released particles is

$$V = \int_v dV = \pi(\alpha + 1)\beta \int_{H_0}^{H+H_0} Z^\alpha \ln \frac{H + H_0}{Z} dZ = \pi h_0^{\alpha+1} \left\{ \left[ \frac{1}{\alpha + 1} \left\langle \frac{H + H_0}{H_0} \right\rangle^{\alpha+1} - 1 \right] - \ln \frac{H + H_0}{H_0} \right\} \tag{8}$$



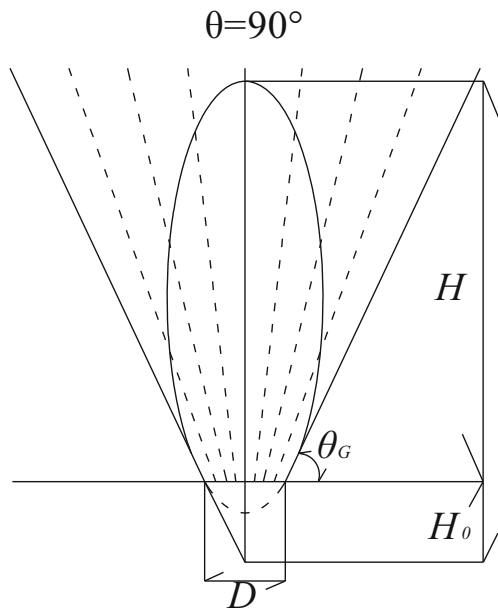


Fig. 4 Relationship between the size of drawpoint and draw body shape

### 5 End Wall Drawing Experiment

It is considered in the stochastic medium theory of gravity flow [19, 21] that due to the double influence of the effective flow size of the ore exit and the end wall surface, the flow parameter values of the particles along the direction of the horizontal and the direction of the vertical inlet are different. As such, the equation of the body surface is given as follows:

$$\frac{y^2}{\beta_1 z^{\alpha_1}} + \frac{(x - kz^{\alpha/2})^2}{\beta \cdot z^\alpha} = (\omega + 1) \ln(H/z) \tag{9}$$

$$\omega = (\alpha + \alpha_1)/2 \tag{10}$$

where  $H$  is the drawbody height, m;  $\alpha$  and  $\beta$  are the granules flow parameters parallel to the access;  $\alpha_1$  and  $\beta_1$  are the granules flow parameters perpendicular to the access;  $k$  is coefficient of flow effected by the solid wall;  $z$  is coordinate in the height direction;  $x$  and  $y$  are the coordinate values of the draw body curve.

In order to obtain each parameter in the above formula, and end wall drawing experiment is designed in which the ore particles are considered to be smaller than 8 mm according to the 1:100 similarity ratio, corresponding to the similarity ratio of the model. The corresponding ore is drawn from the 1050 m mining level of the Yingfangzi silver mine. The

particle size gradation of test particles is shown in Table 2. Taking the laboratory conditions into account, a scaled down model is used to correspond to the large span design of the subsection. The bulk density similarity ratio is 1:1. On the basis of the effective width of ore path in Yangfangzi silver mine, the width of end walls' vent is considered to be 4 m. The vent in the center is opened to avoid the influence of the end wall. The features of the physical test model are as follows: the length of experiment model is 45 cm, the width is 45 cm and the height is 100 cm (see Fig. 5); the marked particle is placed every 5 cm with the distribution shown in Fig. 5.

When placing marker particles, it is very important to ensure that the marker particles are placed in the designed position accurately. Therefore, a positioning plate of marker particles is generally used to fix its position. The positioning plate is shown in Fig. 5a. Marker particles were placed layer by layer (5 cm apart), and the location of marker particles was fixed with the help of positioning plate in each layer. When the filling reaches the predetermined height, the positioning plate is placed lightly on the filling material against the end wall, adjusting the positioning plate to make its center coincide with the axis of the endwall ore draw opening, and then releasing the mark particles into the small round hole of the positioning plate in accordance with its sequence number. After all the marked particles in this layer are released, the positioning plate is gently lifted, and the mark particles are left in their predetermined locations.

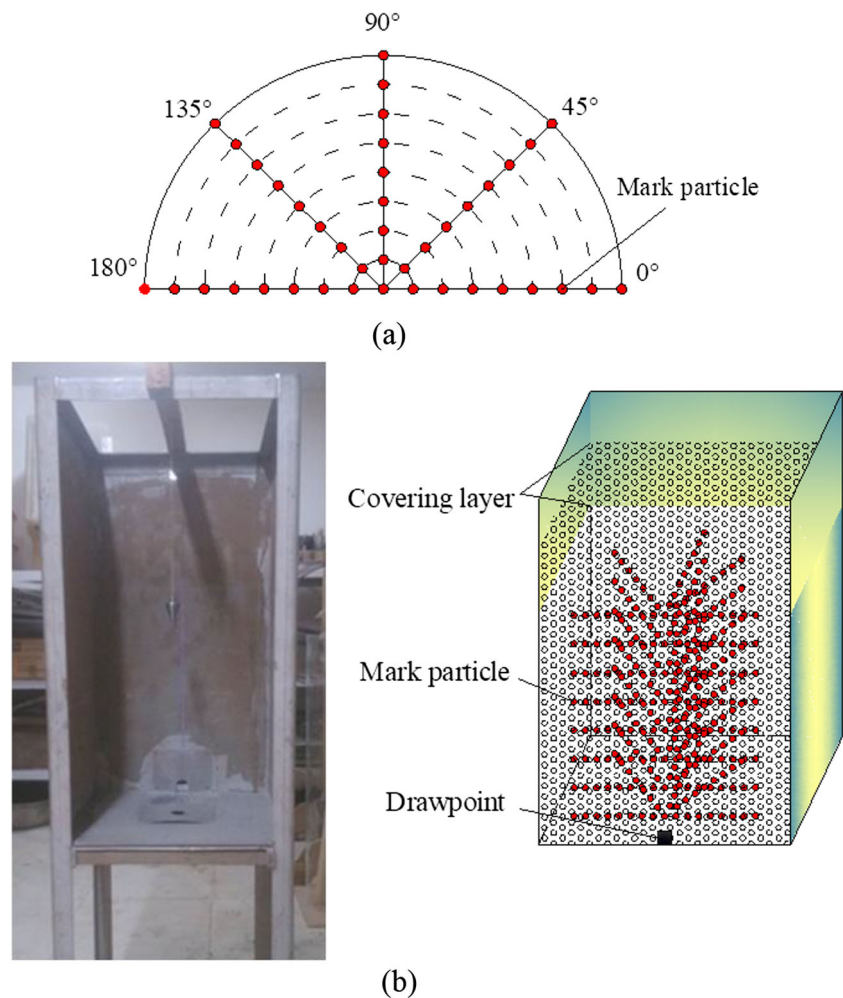
Once the model is completely filled, the material is released from the drawpoint. As particles flow due to gravity, the marked particles arrive at the drawpoint intermittently. The quantity of release between the two marked particles is called the current release quantity. Once the marked particle appears in the drawpoint, the marked particle layer and its point position is recorded and the current release is weighed. The list of the current release quantity values of mark particles at each layer is presented in Table 3, and the release quantity curves are drawn in the coordinate system of quality ( $Q$ ) and radial distance ( $R$ ) in Fig. 6. The longitudinal section shape of the draw body can be obtained by connecting the points with smooth curves. In this way, the shape of the draw body can be obtained by drawing the longitudinal section graph of each azimuth and then drawing the transverse section from these longitudinal section graphs (see Fig. 6).

Based on the longitudinal section of the drawing body obtained from the experiment, a regression fit on the Eqs. (9) and (10) is performed and the flow parameters affected by solid wall drawing experiment are obtained as follows:  $\alpha = 1.548$ ,

Table 2 Particle gradation of loose body

Particle (cm)	<0.2	0.2 ~ 0.3	0.3 ~ 0.4	0.4 ~ 0.5	0.5 ~ 0.6	0.6 ~ 0.7	0.7 ~ 0.8
Percentage (%)	20	15.6	19.7	14.1	17.3	7.2	6.1
Density (g/cm <sup>3</sup> )	1.72						

**Fig. 5** **a** Positioning board for marking particle. **b** Experiment mode of draw body



$\beta = 0.1492$ ,  $k = 0.0851$ ,  $\alpha_1 = 1.4401$ ,  $\beta_1 = 0.1073$ . The correlation coefficient of the regression fitting  $R = 0.9981$ .

Each flow parameter has a different physical meaning, which is embodied in their influence on the shape of the drawbody. Mathematical analysis of Eq. (9) shows that  $\beta$  affects the overall width of the drawbody, and  $\alpha$  determines the relative morphology of the upper and lower part of the drawbody. When  $\alpha < 1/\ln 2$ , the shape of the drawbody is wider at the bottom and narrower at the top. When  $\alpha > 1/\ln 2$ , the shape of the drawbody is wider at the top and narrower at the bottom. When  $\alpha = 1/\ln 2$ , the widest part of the drawbody is in the middle. Therefore, the theory of random medium ore drawing can adapt to the polymorphism of drawbody morphology. The experiment shows that when  $\alpha = 1.548$ , the value is greater than  $1/\ln 2 = 1.4427$ , so the corresponding upper part of the drawbody is wider and the lower part is narrower. According to the experimental data and field investigation, Yingfangzi silver mine is characterized by high viscosity of the ore and poor fluidity of the particles, and the experimental release drawbody is slender.

The physical significance of each flow parameter can be determined by their influence on the shape of the volume

released.  $B$  affects the overall width of the drawbody and  $\alpha$  determines the relative shape of the upper and lower portions of the drawbody. When  $\alpha < 1/\ln 2$ , the lower part of the drawbody is thicker than the upper part. When  $\alpha > 1/\ln 2$ , the upper part of the drawbody is thicker than the lower part. When  $\alpha = 1/\ln 2$ , the widest part of the ejection body is in the middle part. In the experiment,  $\alpha = 1.548 > 1/\ln 2 = 1.4426$ , indicating that the upper part of the drawbody is relatively wide. In the direction of the vertical approach,  $\alpha_1 < 1/\ln 2$  indicates that the ore has a certain degree of viscosity and is suitable for a larger ore drawpoint size.

## 6 A New Method for Determining Optimal Sublevel Height and Drift Spacing

As shown in Fig. 7, since the actual measured shape of the drawbody is a non-standard ellipsoid, it is necessary to deduce a reasonable method for determining stope structural parameters of the non-standard ellipsoid. Figure 6 suggests that segmented drawbodies are only 3 points in

**Table 3** Drawpoint released quantity ( $Q$ ) as a function of level height ( $H$ , [cm]) and horizontal distance ( $R$ , [cm]) from the particle point to the axis of the drawpoint

$\theta = 0^\circ$								
$H$	5	10	15	20	25	30	35	40
$Q_{(R=0)}$	30	97	212	663	895	941	1326	2250
$Q_{(R=1)}$	39		252	608	1111	751	1245	1665
$Q_{(R=2)}$	71	185	309	732	716	798	1227	2070
$Q_{(R=3)}$		1468	1464	656	993	840	1429	3236
$Q_{(R=4)}$			4949	1920	1735	1061	1765	3329
$Q_{(R=5)}$				6513	4931	3766	5253	5514
$Q_{(R=6)}$							9212	9129
$Q_{(R=7)}$								
$Q_{(R=8)}$								
$\theta = 45^\circ$								
$H$	5	10	15	20	25	30	35	40
$Q_{(R=0)}$	30	97	212	663	895	941	1326	2250
$Q_{(R=1)}$	36	115	201	445	866	840	1216	1472
$Q_{(R=2)}$	83	171	272	480	560	808	1237	1536
$Q_{(R=3)}$		614	445	549	663	949	1301	1931
$Q_{(R=4)}$			1543	1179	1192	1613	1598	2031
$Q_{(R=5)}$			3166	2297	1781	2013	2786	2853
$Q_{(R=6)}$				6606	5086	4150	4667	3781
$Q_{(R=7)}$					7102	6895	5529	5276
$Q_{(R=8)}$							9038	8992
$\theta = 90^\circ$								
$H$	5	10	15	20	25	30	35	40
$Q_{(R=0)}$	30	97	212	663	895	941	1326	2250
$Q_{(R=1)}$	30	106	212	421	708	857	1227	1526
$Q_{(R=2)}$	78		299	435	708	879	1709	1586
$Q_{(R=3)}$		694	647	560	1052	1526	1647	1989
$Q_{(R=4)}$			1025	1536	1579	2003	2619	2273
$Q_{(R=5)}$			4599	3521	3166	3108	3283	3131
$Q_{(R=6)}$				5763	4204	5033	5323	4809
$Q_{(R=7)}$					7944	6895	7284	6969
$Q_{(R=8)}$								10,198
$\theta = 135^\circ$								
$H$	5	10	15	20	25	30	35	40
$Q_{(R=0)}$	30	97	212	663	895	941	1326	2250
$Q_{(R=1)}$	46		228	684	908	1086	1730	1969
$Q_{(R=2)}$		449	349	732	1216	1150	1633	2085
$Q_{(R=3)}$		5503	674	1111	1958	2091	2955	2973
$Q_{(R=4)}$			1579	2136	3923	3590	4361	4297
$Q_{(R=5)}$				5276	5416	4723	5813	5703
$Q_{(R=6)}$						7405	10,057	7913
$Q_{(R=7)}$								
$Q_{(R=8)}$								
$\theta = 180^\circ$								
$H$	5	10	15	20	25	30	35	40
$Q_{(R=0)}$	30	97	212	663	895	941	1326	2250
$Q_{(R=1)}$	144	157	222	866	1563	915	1730	2413
$Q_{(R=2)}$	4768	157	421	1253	1735	3483	3440	3022
$Q_{(R=3)}$			2366	4154	4212	7797	7284	7336
$Q_{(R=4)}$				8224	7696	7724		
$Q_{(R=5)}$								
$Q_{(R=6)}$								
$Q_{(R=7)}$								
$Q_{(R=8)}$								

width and tangent, rather than the 5 points and tangent. Therefore, reasonable stope design parameters should be segmented tangent at 3 points if drawbodies are not to overlap each other. When the upper drawing is completed, its space is filled with waste rock filling. When the

drawbody of the next section overlaps with the drawbody of the previous section, it means that the waste rock of the previous section is also released while the ore is being drawn in this section.

The polar equation of drawbody  $R_1$  is defined as:

$$r^2 = (\alpha + 1)\beta Z^\alpha \ln\left(\frac{2H}{Z}\right) \tag{11}$$

where  $Z$  is  $0 < Z < 2H$ . The polar equation of drawbody  $R_2$  is defined as:

$$(r-b)^2 = (\alpha + 1)\beta(Z-H)^\alpha \ln\left(\frac{2H}{Z-H}\right) \tag{12}$$

where  $Z$  is  $H < Z < 3H$ . The polar equation of drawbody  $R_3$  is defined as:

$$r^2 = (\alpha + 1)\beta(Z-2H)^\alpha \ln\left(\frac{2H}{Z-2H}\right) \tag{13}$$

where  $Z$  is  $2H < Z < 4H$ .

If  $R_2$  is tangent to  $R_3$ , the tangent points satisfy both Eqs. (11) and (12), and the slope of the common tangent line

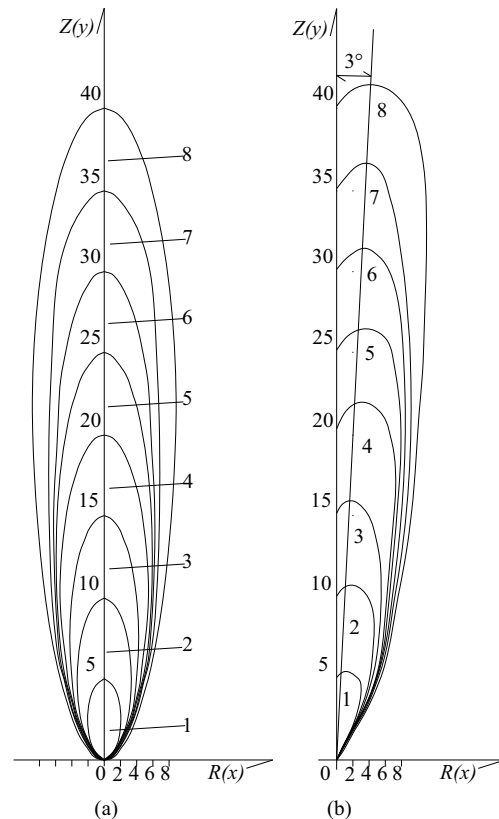


**Fig. 6** Drawing ellipsoid of end drawing experiment. Radial distance ( $R$ /cm) and stratification height ( $Z$ /cm). **a** transverse section; **b** vertical section

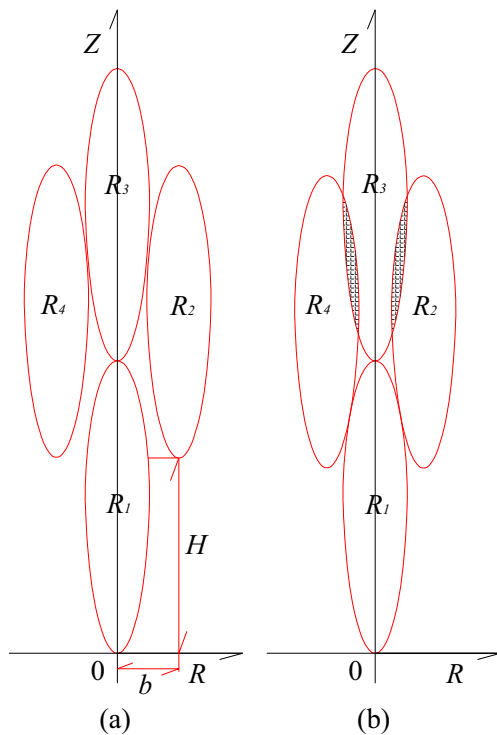


**Fig. 7** Schema of nonstandard ellipsoid tangent in three points. **a**  $R_3$  is tangent to  $R_1$ ,  $R_2$  and  $R_4$ , respectively; **b**  $R_1$  is tangent to  $R_2$ ,  $R_3$  and  $R_4$ , respectively

between  $R_2$  and  $R_3$  is equal, so the following relation set is obtained:

$$\begin{aligned}
 r_2^2 &= (\alpha + 1)\beta(Z_2 - H)^\alpha \ln\left(\frac{2H}{Z_2 - H}\right) \\
 r_3^2 &= (\alpha + 1)\beta(Z_2 - H)^\alpha \ln\left(\frac{2H}{Z_2 - 2H}\right) \\
 \frac{r_2 + r_3}{\frac{dr_2}{dZ_2}} &= \frac{b}{\frac{dr_3}{dZ_2}}
 \end{aligned}
 \tag{14}$$

If  $R_1$  is tangent to  $R_2$ , the tangent points satisfy both Eqs. (11) and (12), and the slope of the common tangent line between  $R_1$  and  $R_2$  is equal, so the following relation set is obtained:

$$\begin{aligned}
 r_1^2 &= (\alpha + 1)\beta Z_1^\alpha \ln\left(\frac{2H}{Z_1}\right) \\
 r_2^2 &= (\alpha + 1)\beta(Z_1 - H)^\alpha \ln\left(\frac{2H}{Z_1 - H}\right) \\
 \frac{r_1 + r_2}{\frac{dr_1}{dZ_1}} &= \frac{b}{\frac{dr_2}{dZ_1}}
 \end{aligned}
 \tag{15}$$

When the flow parameters  $\alpha$ ,  $\beta$  and sublevel height ( $H$ ) are given, one can solve Eqs. (14) and (15) to determine the drawing method. First, the drawbody  $R_1$  and  $R_3$  are made tangent, then, at the level of segment height  $H$ ,  $R_2$  is

drawn and translated to make it tangent to  $R_1$  or  $R_3$ , respectively. Thus, different  $b$  values can be obtained, where the maximum value of  $b$  corresponds to the optimal drift spacing.

When  $\alpha = 1.548$ ,  $\beta = 0.1492$ ,  $H = 10$  m, according to formula (14), it can be obtained that  $Z_2 = 40.73$ ,  $r_2 = 3.97$ ,  $r_3 = 5.76$  and  $b = 7.05$ . Thus, the drift spacing  $B = 2b = 14.10$  m. According to formula (15),  $Z_1 = 21.91$ ,  $r_1 = 1.557$ ,  $r_2 = 4.183$  and  $b = 4.947$ . Thus, the drift spacing  $B = 2b = 9.894$  m. Consequently, when sublevel height  $H = 10$  m, a reasonable drift spacing  $B$  is in the order of  $9.894 \sim 14.10$  m.

The drift spacing has a certain influence on the loss and dilution of the ore, the number of developing workings and their stability. Under general conditions, the drift spacing is mainly determined according to the requirement of fully recovering ore. If the caving ore has a lot of silt and poor fluidity, the flow width is small and a small drift spacing can be used [23, 24]. Conversely, when the drift spacing is too large, the adjacent two stopping drifts are not tangent to the drawbody and the dilution is large. Increasing the drift spacing can increase the residual height of the ridge drawbody, thus increasing the height of the ore heap and the height of the drawbody [25, 26].

The main factors that affect the shape of ore drawbody are ore lumpiness composition (fragmentation), compaction degree, adhesion and humidity etc. [27]. When the lumpiness composition of the ore is fine and compacted, with adhesion and at a certain humidity, the drawing ellipsoid is thin and long, or can even take a tube-like shape. A comprehensive fragmentation measurement program was undertaken during the field experiments. Fragmentation measurement was conducted using high-resolution point data from laser scanning of the draw point muck pile surface, to determine the size of individual rock particles. The particle size distribution was then calculated. A total of 75 laser scans were performed and 54,030 particles were measured. The measured results show that the mean particle size is 163 mm and the proportion of fines (particle size < 50 mm) is 18.6%. Because of the Yingfangzi mine ore’s humidity, viscosities are relatively large, and ore compacts easily. Therefore, the drawbody is thin and long. In this case, when the sublevel height is fixed, the ore loss can be reduced by smaller drift spacing, and it is suggested that the drift spacing is reduced to 10 m.

According to the above analysis, it can be seen that the structural parameters suitable for the Yingfangzi mine are 10 m for sublevel height and 10 m for drift spacing. The adoption of these parameters can maximize the reduction of ore loss and dilution rate and is suitable for the ore properties of the Yingfangzi mine. Figure 8 shows the mining method diagram of sublevel caving method adopting these parameters.



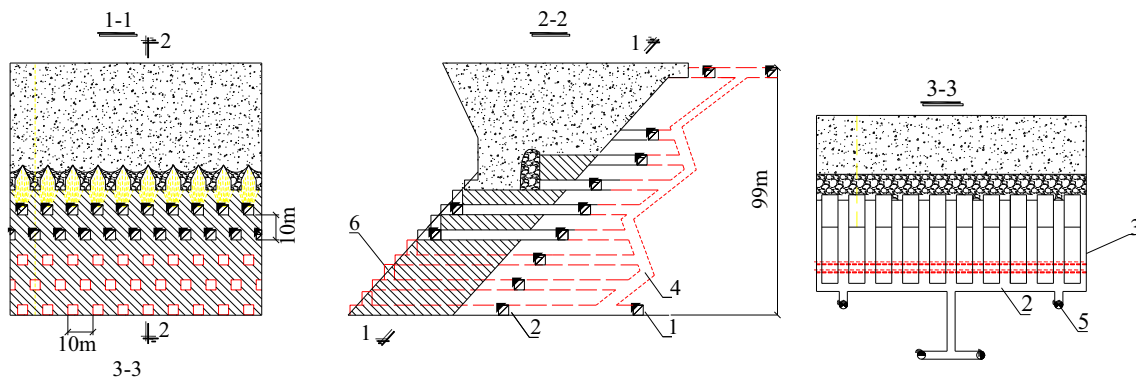


**Fig. 8** Three views of optimal sublevel caving mining schematic: 1,2-Transport drift; 3-Access; 4-Ramp; 5-Ventilating raise; 6-Cut raise

### 7 Optimized Yingfangzi Mine Production

In September 2007, the mine decided to adopt the underground mining method, and started the shaft development for the sublevel caving mine with a production scale of 75,000 tons/year. Subsequently, in August 2012, the mine began partial stoping work. The sublevel height is divided into 13 and 14 m and the drift spacing is chosen at 12.5 m. Mine accesses between upper and lower sublevels are arranged in a staggered manner in diamond shape. Each ore block includes four points of access. 300,000 tons of mined ore resulted in a dilution rate of about 30%, showing that the ore draw is poor. The main reasons of ore dilution are unreasonable assumed parameters, poorly performing technology including poor blasting outcomes.

Since August 2016, in combination with the optimized sublevel caving mining production as described above, the mine has decided to adopt the optimized stope design and carry out field trials with the view to improve production. The trials have achieved good technical and economic benefits. According to the survey of mine production, it was confirmed that the mining recovery rate achieved was about 85% and the dilution rate was about 20%. The dilution rate was 10% lower than previous production. Since the implementation of the new parameters in August 2016, the dilution rate has decreased significantly. During the experiment, the cumulative dilution rate was 18.64%. The monthly variation of the

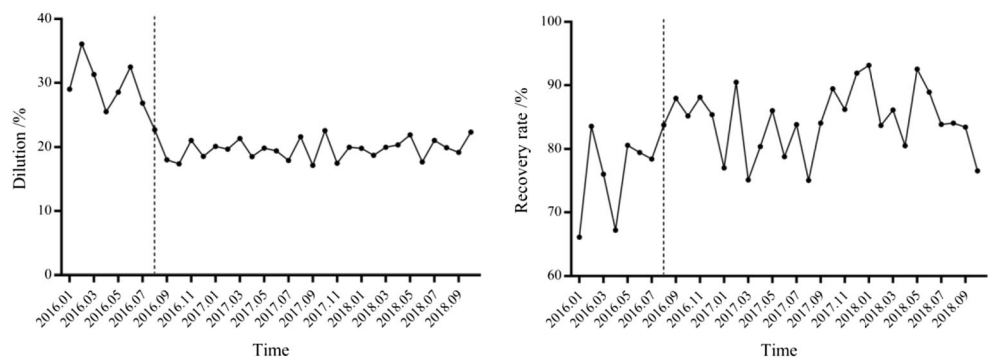
dilution rate is shown in Fig. 9a and of the ore recovery in Fig. 9b.

### 8 Conclusions

This paper presented an alternative method of establishing sublevel cave design parameters for an inclined deposit within a weak rock mass in China. It is observed from the experiment that the release quantity of the particles increases with the size of the drawpoint. The flow parameters of the particles are affected not only by the boundary conditions but also by the size of ore drawpoint. The deficiencies of the existing flow parameter measurement methods for particle materials were analyzed and improved mainly reflected in the following aspects.

Due to the influence of the randomness of particle movement, there is a mismatch in the flow parameter measurement. The flow characteristics and distribution of the marker particles are different from that of the tested particles resulting in large drawbody shape distortion. The flow parameters obtained by the new method are more practical and account for drawpoint width. Furthermore, the new method provides a means to determine the optimum design parameters in sublevel cave mining. It is recommended that the new discharge equation be used to solve the flow parameters in field applications. Also, the new method for determining the stope sub-

**Fig. 9** Percentage dilution (a) and recovery rate (b) for Yingfangzi silver mine



level height should be used when the drawbody is a non-standard ellipsoid. The optimum stope drift spacing can be obtained when all the top drawbodies are tangent to the bottom drawbody at three points.

The optimum design parameters were applied to the Yingfangzi silver mine that has a gently inclined broken soft ore body. The mine optimal values were 10 m for the sublevel height and 10 m for the drift spacing. These values allowed to greatly reduce dilution and improve ore production. The actual production data shows that 85% recovery and 20% dilution was achieved, which resulted in a much better than expected production outcome.

**Acknowledgments** This work was supported by the National Natural Science Foundation of China [grant number 51534003], the Ministry of Science and Technology of the People's Republic of China [grant number 2016YFC0801601] and the China Scholarship Council [grant number 201706080072].

## Compliance with Ethical Standards

**The Conflict of Interest Statement** On behalf of all authors, the corresponding author states that there is no conflict of interest.

## References

- Wagner H (2019) Deep mining: a rock engineering challenge. *Rock Mech Rock Eng* 52:1417–1446. <https://doi.org/10.1007/s00603-019-01799-4>
- Durrheim RJ (2010) Mitigating the risk of rockbursts in the deep hard rock mines of South Africa: 100 years of research. Society for Mining, Metallurgy, and Exploration, Inc., ISBN 978-0-87335-322-9, pp 156–171
- Bull G, Page CH (2000) Sublevel caving—today's dependable low-cost 'ore factory'. *MassMin 2000 Proceedings*. Brisbane: The Australasian Institute of Mining and Metallurgy, pp 537–556
- Wilson AH (1983) The stability of underground workings in the soft rocks of the coal measures. *Int J Min Eng* 1:91–187. <https://doi.org/10.1007/BF00880785>
- Castro R, Pineda M (2015) The role of gravity flow in the design and planning of large sublevel stopes. *J South Afr Inst Min Metall* 115(2):113–118. <https://doi.org/10.17159/2411-9717/2015/v115n2a4>
- Hustrulid W, Kvapil R (2008) Sublevel caving—past and future. *Proceedings of the 5th international conference and exhibition on mass mining*, Luleå University Press, Luleå, pp 107–132
- Woodruff SD (1966) *Methods of working coal and metal mines: planning and operations*, M. Elsevier
- Mudd GM, Jowitt SM, Werner TT (2017) The world's by-product and critical metal resources part I: uncertainties, current reporting practices, implications and grounds for optimism. *Ore Geol Rev* 86: 924–938. <https://doi.org/10.1016/j.oregeorev.2016.05.001>
- Zhang ZX (2016) Failure of hanging roofs in sublevel caving by shock collision and stress superposition. *J Rock Mech Geotech Eng* 8(6):886–895. <https://doi.org/10.1016/j.jrmge.2016.06.005>
- Jaak JK Daemen (2003) Mining Engineering. *Encyclopedia of Physical Science and Technology* (Third Edition) pp 65–96. <https://doi.org/10.1016/B0-12-227410-5/00871-1>
- Freidin AM, Neverov SA, Neverov AA, Filippov PA (2008) Mine stability with application of sublevel caving schemes. *J Min Sci* 44(1):82–91. <https://doi.org/10.1007/s10913-008-0008-z>
- Brady B, Brown E (2007) Longwall and caving mining methods. *Rock mechanics for underground mining*, pp 430–483. [https://doi.org/10.1007/978-1-4020-2116-9\\_15](https://doi.org/10.1007/978-1-4020-2116-9_15)
- KumarHaldar S (2018) Chapter 12 - Elements of Mining. *Mineral Exploration* (Second Edition) Principles and Applications, pp 229–258. <https://doi.org/10.1016/B978-0-12-814022-2.00012-5>
- Tao GQ, Lu MX, Zhang XF, Zhang R, Zhu ZH (2019) A new diversion drawing technique for controlling ore loss and dilution during longitudinal sublevel caving. *Int J Rock Mech Min Sci* 113: 163–171. <https://doi.org/10.1016/j.ijrmms.2018.12.006>
- Brunton ID, Fraser SJ, Hodgkinson JH, Stewart PC (2010) Parameters influencing full scale sublevel caving material recovery at the ridgeway gold mine. *Int J Rock Mech Min Sci* 47(4):647–656. <https://doi.org/10.1016/j.ijrmms.2009.12.011>
- Martinez MA, Newman AM (2011) A solution approach for optimizing long - and short-term production scheduling at LKAB's Kiruna mine. *Eur J Oper Res* 211(1):184–197. <https://doi.org/10.1016/j.ejor.2010.12.008>
- Castro RL, Fuenzalida MA, Lund F (2014) Experimental study of gravity flow under confined conditions. *Int J Rock Mech Min Sci* 67:164–169. <https://doi.org/10.1016/j.ijrmms.2014.01.013>
- Bustillo RM (2018) Mineral Resource Extraction. *Mineral Resources*. In: Springer Textbooks in Earth Sciences, Geography and Environment. Springer, Cham, pp 311–421. [https://doi.org/10.1007/978-3-319-58760-8\\_5](https://doi.org/10.1007/978-3-319-58760-8_5)
- Ren FY (1994) *The stochastic medium method of ore-drawing and its application*. Metallurgical Industry Press, Beijing (in Chinese)
- Melo F, Vivanco F, Fuentes C (2009) Calculated isolated extracted and movement zones compared to scaled models for block caving. *Int J Rock Mech Min Sci* 46(4):731–737. <https://doi.org/10.1016/j.ijrmms.2008.09.012>
- Ren FY (1992) *Theory and practical application of random medium for ore drawing*. Northeast University, Shenyang (in Chinese)
- Tao GQ, Ren FY, Liu ZD et al (2010) Research on improvement of the stochastic medium theory for ore drawing. *J Min Saf Eng* 27(02):239–243 (in Chinese)
- Wimmer M (2010) *Gravity flow of broken rock in sublevel caving (SLC) – state-of-the-art*. Luleå University of Technology, Luleå
- Johansson D, Ouchterlony F (2011) Fragmentation in small-scale confined blasting. *Int J Min Miner Eng* 3(1):72–94. <https://doi.org/10.1504/ijmme.2011.041450>
- Brady BHG, Brown ET (2004) *Rock mechanics for underground mining*, 3rd edn. Kluwer, Dordrecht
- Power GR (2004) *Modelling granular flow in caving mines: large scale physical modelling and full scale experiments*, PhD thesis, University of Queensland
- Janelid I, Kvapil R (1966) Sublevel caving. *Int J Rock Mech Min Sci Geomech Abstracts* 3(2):129–153. [https://doi.org/10.1016/0148-9062\(66\)90004-0](https://doi.org/10.1016/0148-9062(66)90004-0)

**Publisher's Note** Springer Nature remains neutral with regard to jurisdictional claims in published maps and institutional affiliations.